Seismic Behavior of Semi-Dry Precast Concrete Connections Using Tapered Thread Couplers

E. Mobedi[1], H. Parastesh[1*], and A. Khaloo[2]

1. Department of Civil Engineering, University of Science and Culture, Tehran, Iran
2. Department of Civil Engineering, Sharif University of Technology, Tehran, Iran

Corresponding author: *parastesh@usc.ac.ir*

ARTICLE INFO

ABSTRACT

The worldwide usage of precast concrete frames leads to an increase in the need for the investigation of efficient precast connections, particularly in the seismic regions. The current paper provides a numerical and experimental study on a dry precast connection. Experiments were conducted with the aim to validate the finite element method in the laboratory of the University of Science and Culture. In order to verify the validity of the result, the outcomes of the non-linear analysis of cross-shaped models were compared to the experimental results in terms of failure mode, ductility, lateral load-bearing capacity, and energy dissipation. The finite element non-linear analyses of the models represented an acceptable compatibility with experimental results. A parametric study has been carried out to survey the effect of the couplers and grout compressive strength on semi-dry connection behavior. Eventually, the response modification factors were determined for the case studies to demonstrate the seismic behavior in design forces. Statistical analysis of the numerical results demonstrates a 6 % increase in response modification factors of the specimens with the closest distance of couples to the column face in relation to those with the couplers farthest away from the column face. Eventually, it can be concluded that the specimens with a shorter coupler distance from the external face of the column and with a higher grout compressive strength lead to the appropriate results.

1. Introduction

Generally, precast concrete members can be applied as the structural members of a building and non-structural ones, e.g. the facade or separating walls. The major advantages of precast members are rapid installation, lower cost, and higher quality. The safety and resistance of the precast structures are mostly depending on their

connections. If no lateral load-bearing system is utilized, therefore the beam-column connection must be designed as a moment-resisting connection. The precast connection method involves some limitations such as an essential need for precise molding, accurate installation of special cranes, and equipment of construction. In spite of extensive studies on beam-column connections, a limited number of them focused on the rigid precast concrete beam-column connection.

A laboratory study was conducted on the behavior of 10 specimens of integrated concrete internal beam-column connection [1]. Main variables of this study included the amount and type of pre-stressed and non-prestressed steel. An experimental study was conducted on three full-scale specimens of the precast external beam-column connections [2]. An important parameter was the formation of plastic hinge at the internal face of the beam.

Too many efforts have been made to investigate the rigid beam-column connection using anchored steel plates in concrete [3-5]. In a research project performed using the PCI, eight simple and eight moment-resisting beam-column connections were studied and tested in Washington University [6]. This program aimed to evaluate various method of connecting precast construction members based on economic and design-related considerations.

Tankat et al. proposed several pre-cast connections [7] and the results of tests were compared to a monolithic specimen, indicating that the pre-cast specimens can compete with cast-in-place ones in terms of strength, ductility, and energy dissipation.

Khaloo and Parastesh conducted studies on precast moment-resisting beam-column connections [8, 9]. Parastesh et al. carried out several researches on connections for both concrete and steel material [10,11]. For instance, Parastesh et al. tested the eight specimens of moment-resisting beam-column semi-dry connections [10]. IN consonance with the test results, the proposed pre-cast connection provided the required flexural strength, ductility, energy dissipation.

Kulkarni et al. introduced an innovative precast connection. The proposed connection was performed using nuts and bolts in accordance with steel plates placed inside the beam and column. Several numerical models of proposed connection were simulated applying the finite-element DIANA software to study seismic behavior [12].

Guan et al. introduced a new method for replacing high-resistance reinforcement bars in precast connections in order to prevent the congestion of bars at the connection zone. Several states of using high-resistance bars in lower bars of the beam restrained at the connection zone were tested. The invented connection had a satisfactory performance in seismic loadings. Moreover, the embedment of the lower bars at the connection zone can be neglected [13].

Bahrami et al. proposed a precast connection consist of a continuous column and two corbels connected to beams. These corbels were connected to the connection parts provided below the beams applying screws or welding. Results of the parametric studies on the carried out connection demonstrate that the connection response includes the strength, ductility, rigidity, and energy dissipation can reach approximately 80% of the monolithic constructed connections [14].

Fathi et al. invented a type of metal connection consist of welded metal plates and gussets in order to connect the precast continuous concrete column to the semi-precast concrete beams. This connection was connected to the beam using screws or welding. In consonance with the numerical and experimental results, this connection demonstrates a performance similar to that of the monolithic constructed connection [15].

Xiao et al. introduced a dowel pin connection applying a stepped form corbel connected to the precast column. They also utilized recycled concrete in the test specimens. In addition to the suitable seismic performance, the bolted connection facilitates deconstruction and replacement of members [16].

Yan et al. provided precast connections by considering the holes for the passage of bars in precast continuous beam members. The couplers were implemented as the couplers of bars. As the failure mode and plastic hinge formation of this connection depends on the slippage of bars, type of grout, array of the holes, and the couplers arrangement, the seismic behavior of the connection is not similar to the monolithic constructed connection [17].

Alias et al. conducted an experimental program to inquire the performance of grouted sleeve connectors in different conditions. Too many load displacement curves can be extracted from their studies for applying in precast joint performance studies [18].

Clementi et al. inspected the application of dowel pin connection in a concrete framed industrial building. The nonlinear numerical analyses were performed under ten earthquake inputs applying different aspects of material nonlinearity in the models. their study results proved that consideration of the issues related to new precast systems play fundamental role in the dynamic performance of precast reinforced concrete frames [19].

Nzabonimpa et al focused on the finite element simulation of the experimental responses in the precast joint performance domain. The main part their research was about end plate connection methods in the precast concrete joints. Eventually, they compared the effects of the different material nonlinearity method in the accuracy of the ABAQUS software predictions of the experimental responses [20].

Girgin et al. explored the seismic behavior of precast moment resisting frames. They selected a semi dry connection with a detail consists of the column corbels, grouted parts and steel plates under beam parts. Several incremental dynamic analyses were performed to investigate the response modification factors (R) in the three to five stories precast concrete buildings. Their study results proved that the R factors was less than that of presented by the code provisions for the selected precast connection [21].

Bompa and Elghazouli extracted more than 350 specimens with different types of couplers from the former studies reports to compare their performance in terms of energy dissipation, ductility, and strength. Their study results prove that PTC (parallel thread coupler) provides the most efficient connection from the structural and constructional point of view [22].

Woon et al. conducted an experimental and numerical program to inspect the role of high damping rubber (HDR) in the performance of

the precast beam to column connection. In their proposed connection, the protruding end of the precast beam has been pulled in the prefabricated depression of the column corbel. The corbel depression has been also lined with a layer of HDR to form a damping connection. Their study results revealed that although the maximum cyclic bearing capacity and the strength ratio of the joint is a little less than monolithic specimen, the energy dissipation of the connection is ameliorated [23].

In the current study, a new assembly of precast semi-dry connection is provided. The seismic behavior of the proposed connection is evaluated through the extensive numerical and experimental studies. Different arrangements of the couplers have been considered to study the seismic performance of the connection zone in the terms of the rigidity, ductility and energy dissipation variables. The key role of the grout compressive strength on the connection behavior was determined pursuant to experimental observations and ABAQUS software output data.

2. Numerical Models Features

The numerical models dimensioned based on the test specimen of the precast middle joint with actual scale. The details of the cat-in-place and precast models for middle joints are portrayed in Figures 1 and 2. The precast connection was designed by assuming the behavior of the monolithic constructed connection. Figure 3 presents a 3D model of the BC-3 specimen whose features are presented in Table 1.
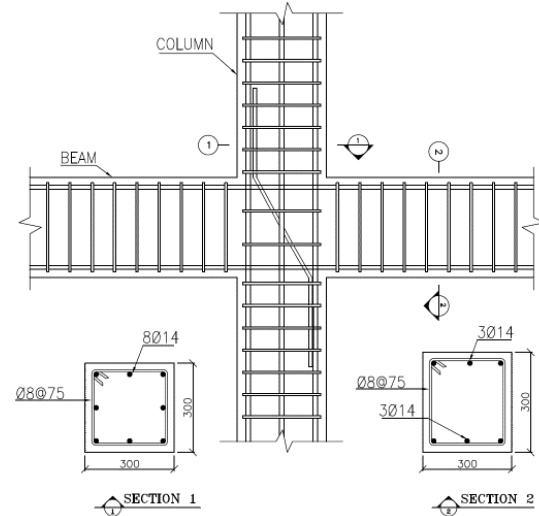

Fig. 1. The monolithic constructed middle joint (dimensions are in mm).
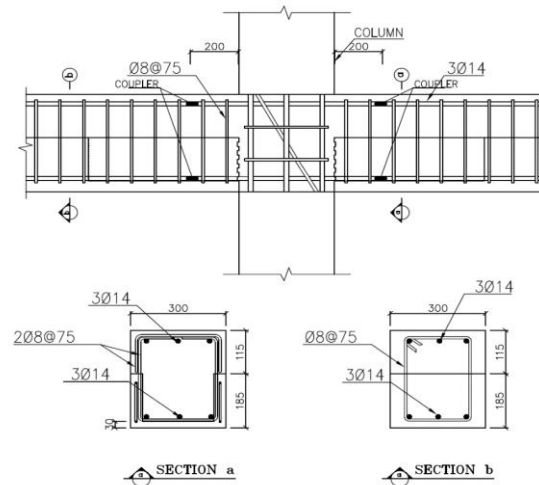

Fig. 2. The precast middle joint (dimensions are in mm).

All specimens were tested under the constant axial load (10% axial load-bearing capacity of the column) and lateral cyclic loading on the column. In Figure 4, the loading, boundary conditions and length of beam and column members in the middle joints are illustrated. The lateral load was applied based on the load increments until the end of the elastic stage, and then load controlled cycles were converted to displacement controlled one (Figure 5).
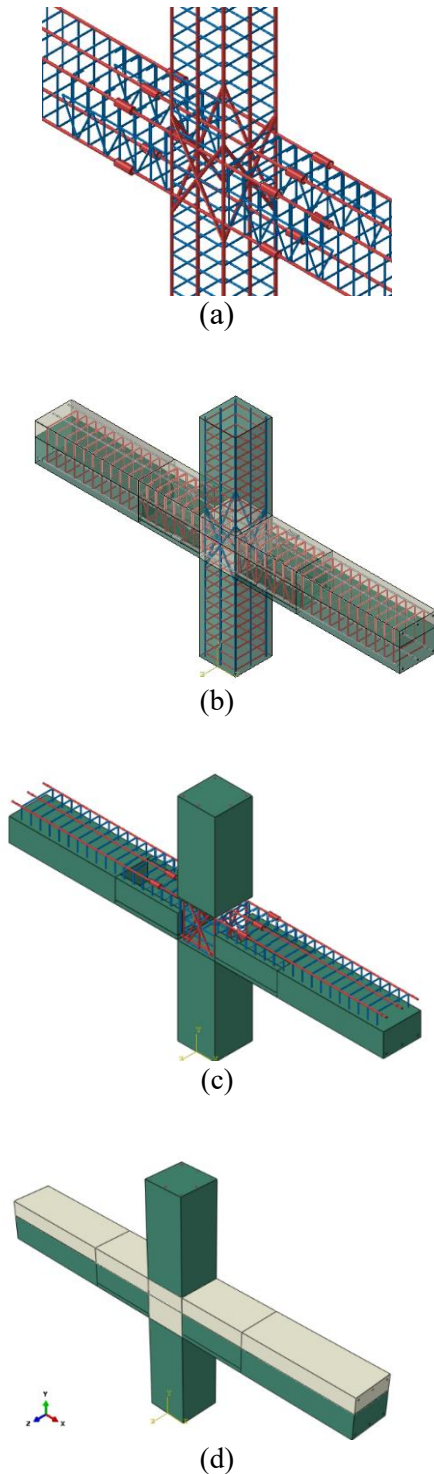
(a)

(b)

(c)

(d)

Fig. 3. The 3D model of B C-3; a) Couplers and diagonal reinforcement of the column b) Reinforcement arrangement in the dry (precast) and wet (cast in place) parts c) Dry (precast parts) d) Complete dry (precast) and wet (cast in place) parts.
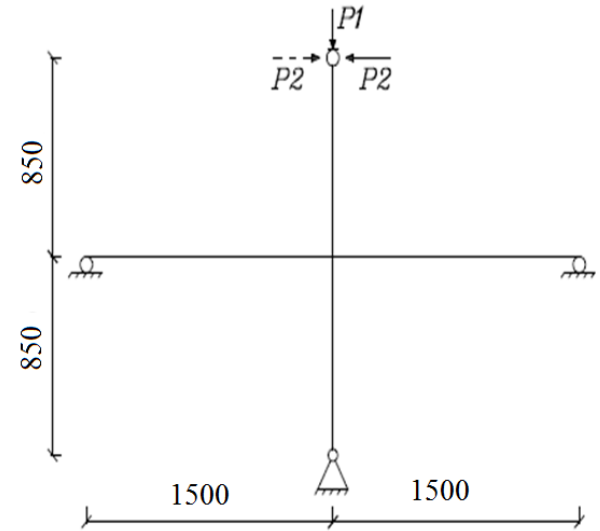

Fig. 4. Type of loading and boundary conditions (dimensions are in mm).
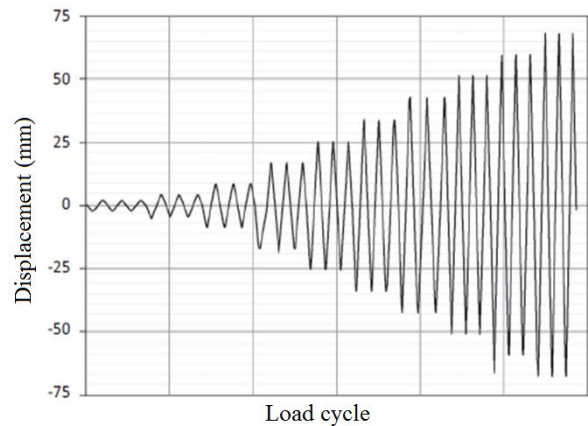

Fig. 5. Cyclic lateral load protocol.

A summary of the features of models applied in this study is depicted in Table 1. The BC1 model is the observant one (monolithic model with no couplers). BC2 to BC17 models are classified in terms of the array of couplers, stirrup distance, and axial load intensity. In BC2 to BC5, the distance of coupler to the column face were set to 20 cm, this distance is decreased to 5 cm in BC6 to BC10. In BC10 to BC13, overlap splices replaced by couplers at the bottom layer of reinforcement, and in BC14 to BC17, couplers were placed in different 5- and 20 cm arrangements.

Table 1. Details of the numerical models.

Model name	Normal concrete MPa	Grout MPa	Notes
BC1	25	-	Beam and column are cast in-place (monolithic constructed specimen)
BC2	25	30	Connection zone is grouted, and the location of the couplers is 20 cm from the column face.
BC3	25	35	Connection zone is grouted, and the location of the couplers is 20 cm from the column face.
BC4	25	30	Connection zone is grouted, the location of the couplers is 20 cm from the column face, and the axial compressive force is halved.
BC5	25	30	Connection zone is grouted, the location of the couplers is 20 cm from the column face, and the stirrup distance is decreased.
BC6	25	30	Connection zone is grouted, and the location of the couplers is 5 cm from the column face.
BC7	25	35	Connection zone is grouted, and the location of the couplers is 5 cm from the column face.
BC8	25	30	Connection zone is grouted, the location of the couplers is 5 cm from the column face, and the axial compressive force is halved.
BC9	25	30	Connection zone is grouted, the location of the couplers is 5 cm from the column face, and the stirrup distance is decreased.
BC10	25	30	Connection zone is grouted, the location of the couplers is 5 cm from the column face, and the bottom layer bars contain overlap splices.
BC11	25	30	Connection zone is grouted, the location of the couplers is 20 cm from the column face, and the bottom layer bars contain overlap splices.
BC12	25	30	Connection zone is grouted, the location of the couplers is 20 cm from the column face, the bottom layer bars contain overlap splices, and the compressive axial force is halved.
BC13	25	30	Connection zone is grouted, the location of the couplers is 20 cm from the column face, the bottom layer bars contain overlap splices, and the stirrup distance is decreased.
BC14	25	30	Connection zone is grouted, and the location of the couplers is 5 cm and 20 cm from the column face in different arrays.
BC15	25	35	Connection zone is grouted, and the location of the couplers is 5 cm and 20 cm from the column face in different arrays.
BC16	25	30	Connection zone is grouted, the location of the couplers is 5 cm and 20 cm from the column face in different arrays and the axial compressive force is halved.
BC17	25	30	Connection zone is grouted, the location of the couplers is 5 cm and 20 cm from the column face in different arrays, and the stirrup distance is decreased.

3. Finite Element Method

For 3D modeling and non-linear analysis of the reinforced concrete connections, the ABAQUS software was applied. Moreover, the conventional elastoplastic model was deliberated to define the behavior of steel. The modulus elasticity, the Poisson's coefficient and the yield stress of the steel bar material were assumed to be 204000 MPa, 0.3 and 470 MPa, respectively. The density, the elasticity module, and Poisson's ratio of

the concrete material were assumed to be 2400 kg/m³, 23400 MPa of 0.2, respectively. The concrete damage plasticity (CDP) model was applied in order to contemplate a non-linear behavior for the concrete [24]. This model is appropriate for concrete under dynamic or cyclic loading as well as static loading. In this model, two major failure mechanisms of concrete, i.e. tensile cracking and compressive crushing, were considered. The compressive behavior of concrete is modified to consider the confinement effects of the transversal reinforcement steels pursuant to the procedure proposed by Mander [25] (Figure 6). The CDP constitutive material low considers the tensile behavior of the concrete after tensile failure. The tensile strength of concrete is assumed to be 10 percent of the concrete's uniaxial compressive strength, i.e. 2.5 MPa. The post-failure strain is contemplated for a strain ranges about ten times of the ultimate elastic strain. The effects of interactions between concrete and reinforcement steel are considered applied the definition of the post-failure behavior of concrete. Therefore, the bond-slip effects are deliberated between reinforcement steel and concrete, such that, after the tensile failure of the concrete parts, the load is transferred from cracks to reinforcement steels [24].
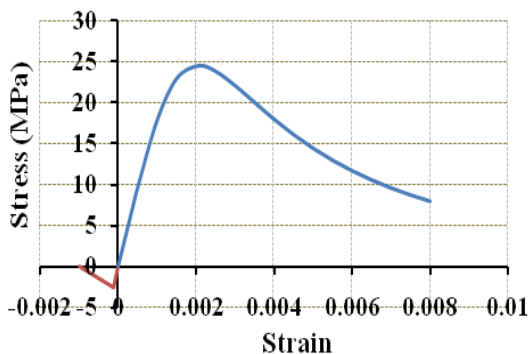

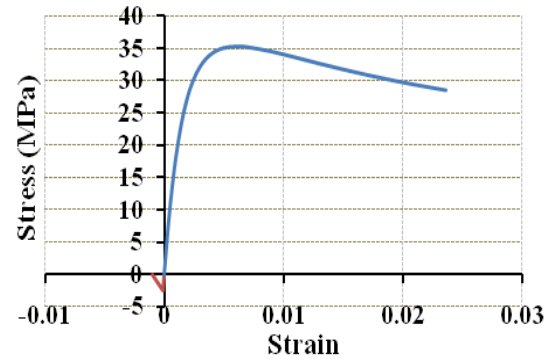**Fig. 6.** The stress-strain curve of the confined concrete [25].

Fig. 7. The stress-strain curve of the unconfined concrete [25].

The mentioned potential function for the plastic behavior of the concrete is the Drucker-Prager hyperbolic equation. Furthermore, the Lubliner yield surface with modifications proposed by Lee and Fenves are considered for definition of the constitutive material law [24,26] (see Figure 7).

The dynamic explicit non-linear method was performed to analyze of the connection behavior. The selected method applies the central-difference rule for solving non-linear equations. In contrast to implicit solution method, the explicit methods do not require estimating the response in the next step time (t+Δt), therefore there is no need to trial and error process and also convergence tolerance. Figures 4 and 5 display loading type and boundary conditions. The eight-node reduced integrated cubic elements C3D8R were selected for the concrete parts. The dual-node 3D truss element T3D2 was applied for reinforcement bars and couplers. The couplers were modeled as a part of bars associated with more cross-sectional area.

The reinforcement element nodes were constrained to the closest nodes of the C3D8R elements of the concrete parts by means of the "Embedded elements" technique [24]. Figure 8 presents a schematic description of embedded region technique in ABAQUS software. The preferred mesh size of the elements was assumed to be 30 mm for concrete and bar elements. The mesh dimensions were calibrated in agreement with the test results.
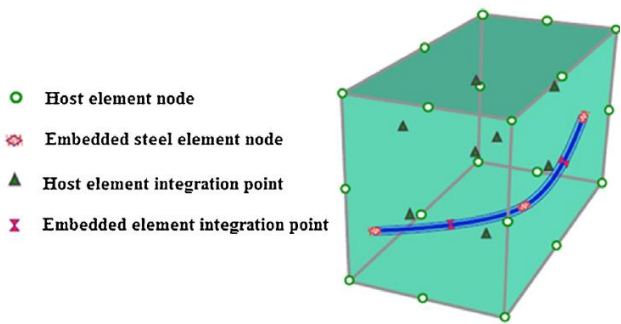

Fig.. 8. Embedded region technique [24].

4. FE Method Verification

4.1. Parastesh et al. Studies

Parastesh et al. [10] conducted extensive experiments on the connection proposed in Figure 9. In the present study, results of these numerical studies were used to verify the finite-element method.

Test specimens were comprised of precast concrete with the compressive strength of 22 MPa, cement slurry (as the filler and complementing the precast connection) with the compressive strength of 23 MPa, and closed stirrups with the distance of 75 cm.

Figure 10 presents test set-up, loading type, and boundary conditions of the test.
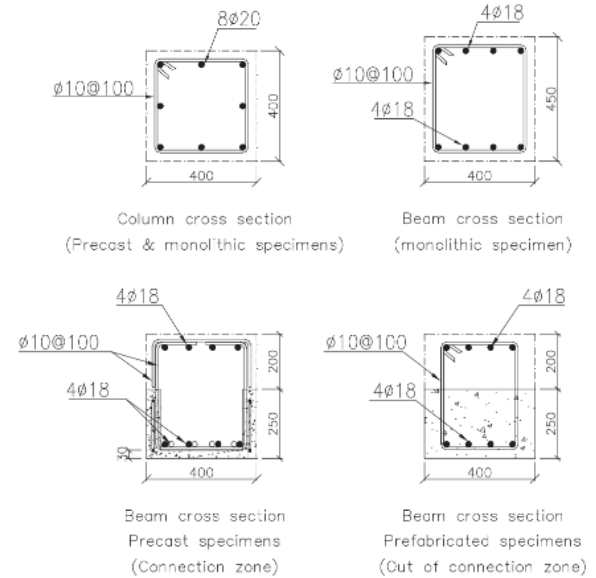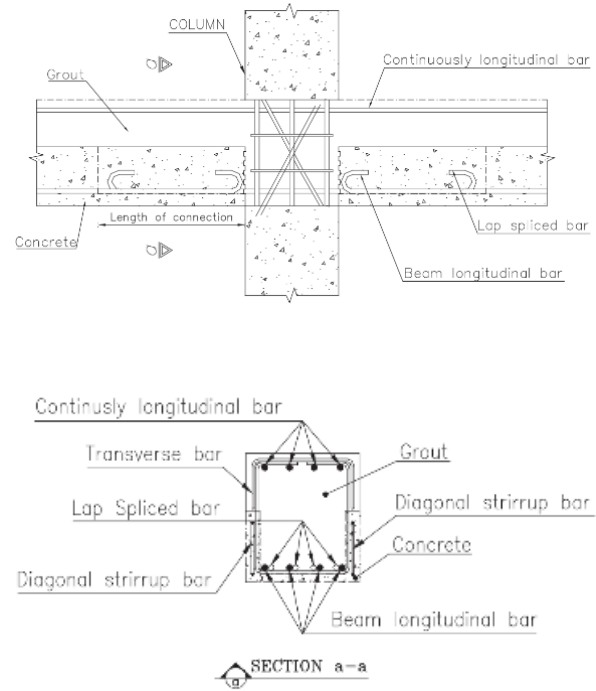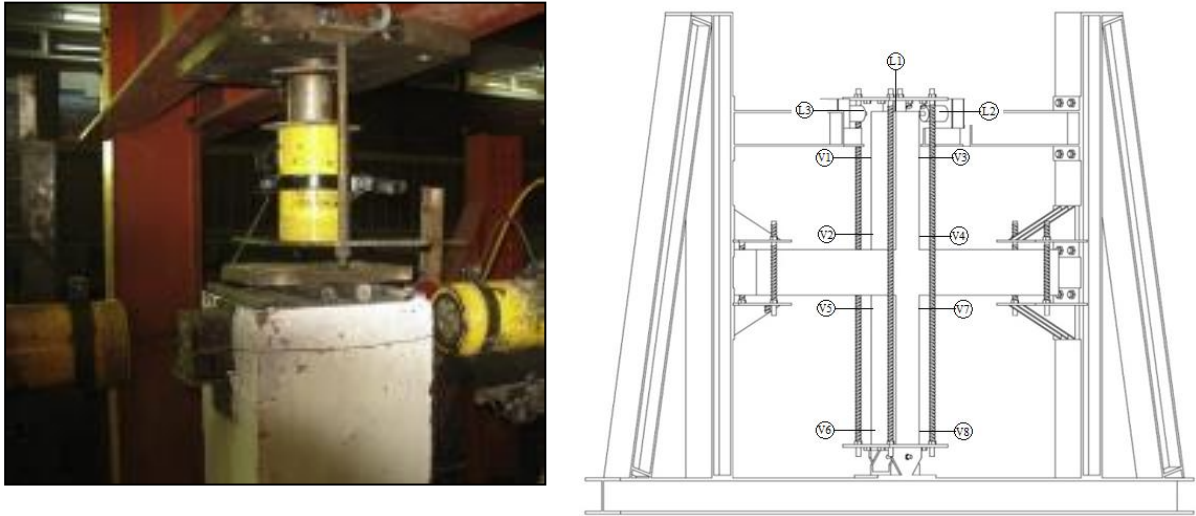

Fig. 9. Test specimen of Parastesh et al. [10].

Fig. 10. Test set-up of the experiment performed by Parastesh et al. [10].
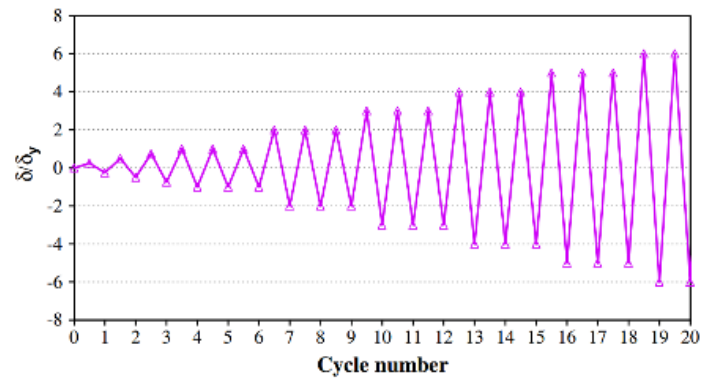

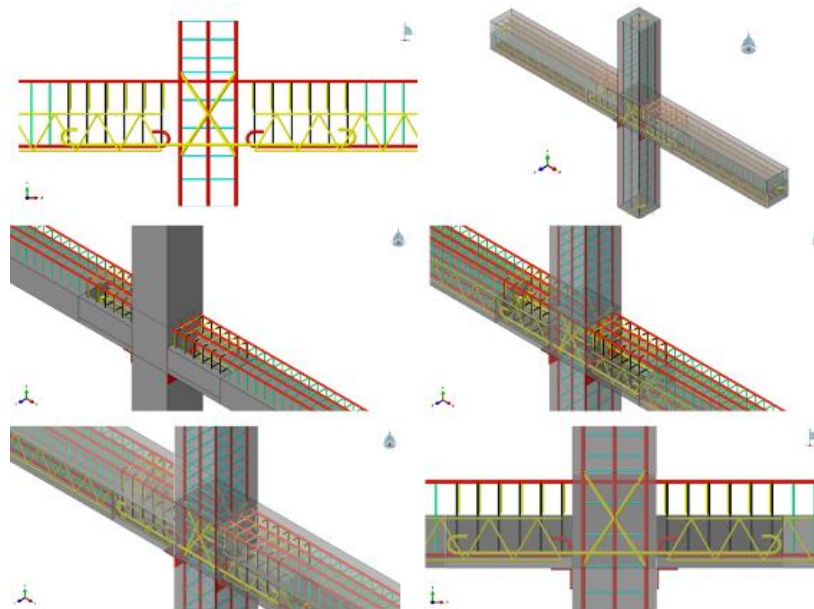**Fig. 11.** Cyclic loading of the experiment performed by Parastesh et al. [10].

Fig. 12. a Numerical model of the test specimen of Parastesh et al. [10].
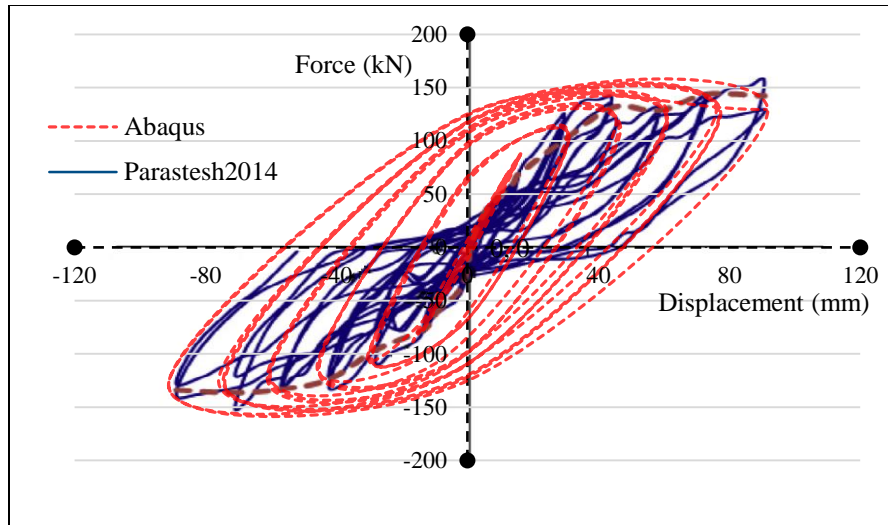
Fig. 13. Load-displacement hysteresis of the precast connection.

The cyclic loading protocol of these experiments is given in Figure 11. The components of the numerical models are illustrated in Figure 12.

The final load-bearing capacity, maximum displacement, displacement of connection at the end of the elastic region (yield displacement), and ductility coefficient (ratio of failure displacement to yield displacement) were compared through numerical and test results (Figure 13.). The maximum load-bearing capacity and maximum deformation of the test specimen are equal to 161.3 KN and 103.7 mm, respectively. The numerical model of the test specimen was simulated in ABAQUS by deliberating the full details of reinforcement steels, precast, and cast in-place parts.

The numerical model of the laboratory specimen of Parastesh et al. demonstrates the maximum displacement of 104.9 mm and final load-bearing capacity of 158.2 kN. Thus, the deviation of the results of the

numerical model compared to the test results is about 1.9%, indicating a good compatibility of the numerical and experimental results. The areas under the envelope of hysteresis curves were determined for the numerical model and the test specimen. The comparison of the later criteria reveals a little more deviation around 7%. The main reason of the result deviation is the lack of capability of the software in simulation of the pinching effects. As the CDP material model is not applicable for simulation of the pinching effect, the deviation of the results in the later criteria are slightly higher than the mentioned ones. This fact can be observed in the numerical results presented by Ab-Kadir et al. [27].

4.2. The University of Science and Culture Experiment Program

The BC3 model was selected to construct a half scale test specimen. The main purpose of the experimental program is to determine the effect of the coupler's arrangement in the semi-dry precast connection zone.
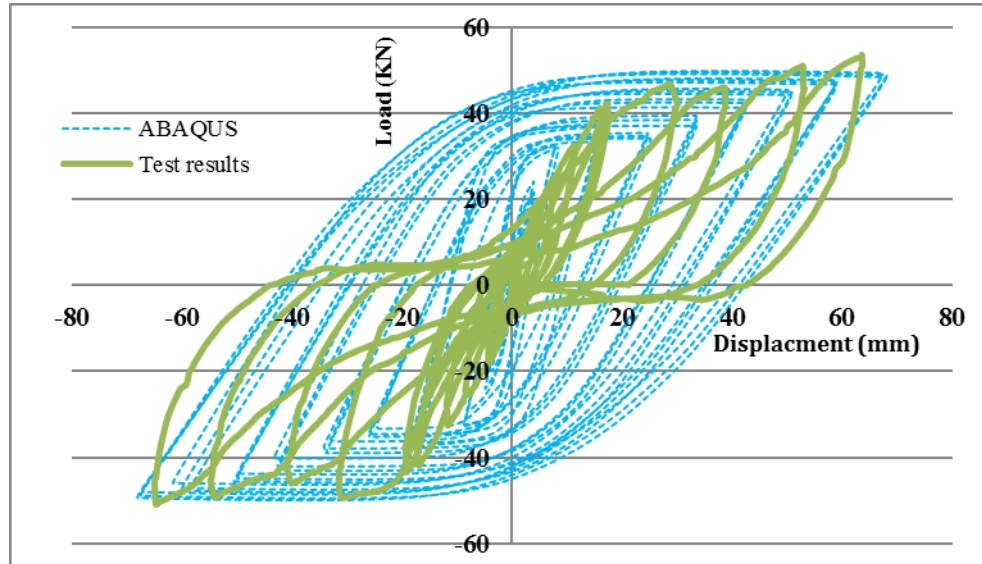
Fig. 14. Load-displacement hysteresis of the BC3 specimen.

Figure 14 compares the numerical and test results of load-displacement hysteresis of the BC-3 specimen. The comparison of the results leads to same deviations as obtained through the FE method verification with Parastesh et al. test studies results.

The concrete damage plasticity was applied to visualize the crack propagation of the connection zone in the numerical models output. Generally, the prediction of the main modes of failure is essential for exact perception of the seismic behavior of the precast connection zone. The vertical cracks were initiated in the beams, and subsequently the flexural cracks were also appeared in the column by increasing the amplitude of the load cycles. The flexural cracks in the vicinity of the connection zone were transformed to shear cracks. Figure 15

presents the comparison of the cracking pattern of the BC3 model in the laboratory and ABAQUS software.
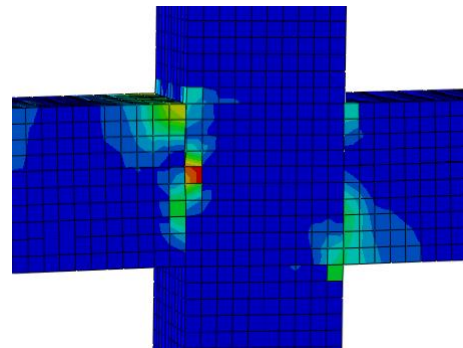

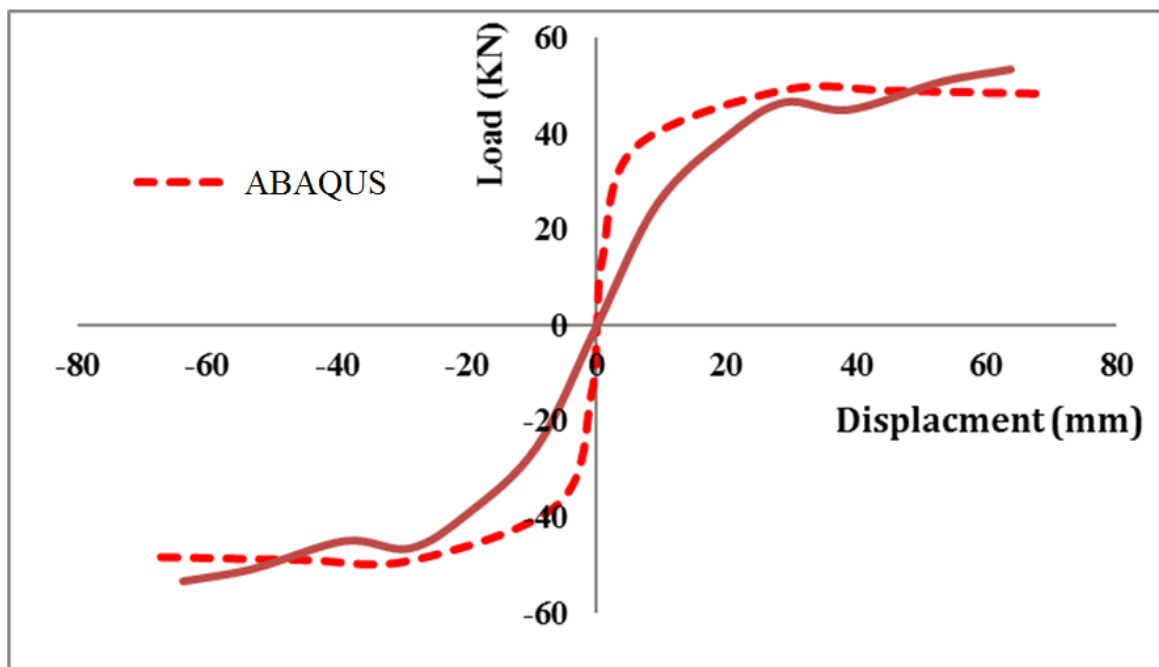**Fig. 15.** Crack propagation in the BC3 model.

Fig. 16. Load-displacement envelope of the BC3 model.

Figure 16 provides the load-displacement envelope of the hysteresis curve displayed in Figure 13. The value of yield displacement equals to 17.28 and 18.31 mm in numerical and test results, respectively. The ductility coefficient was obtained as 3.02 and 2.85 for the numerical and test results, respectively. Less than 7 % deviation of the numerical and experimental results proves the capability of the FEM method. As illustrated in Figure 16, the envelope of load-displacement hysteresis resulted from the BC3 numerical model reveals a good agreement with the test results.

5. Results and Discussion

Figure 16 presents the load-displacement hysteresis of some of the selected models.

The models were selected consciously to highlight the differences of the numerical models. Figure 16 also displays the envelope of the hysteresis curves. The coefficients relevant to the seismic behavior were calculated applying the envelope curve properties. The crack propagation pattern captured from the numerical visualized output data is so similar to the test observations. The flexural cracks were initiated in the beam member, and then the cracks were appeared in the column surface. The vertical flexural cracks were converted to inclined flexural-shear cracks in the vicinity of the connection zone. Figure 17 demonstrates the cracking pattern in the numerical models of BC13 and BC14.
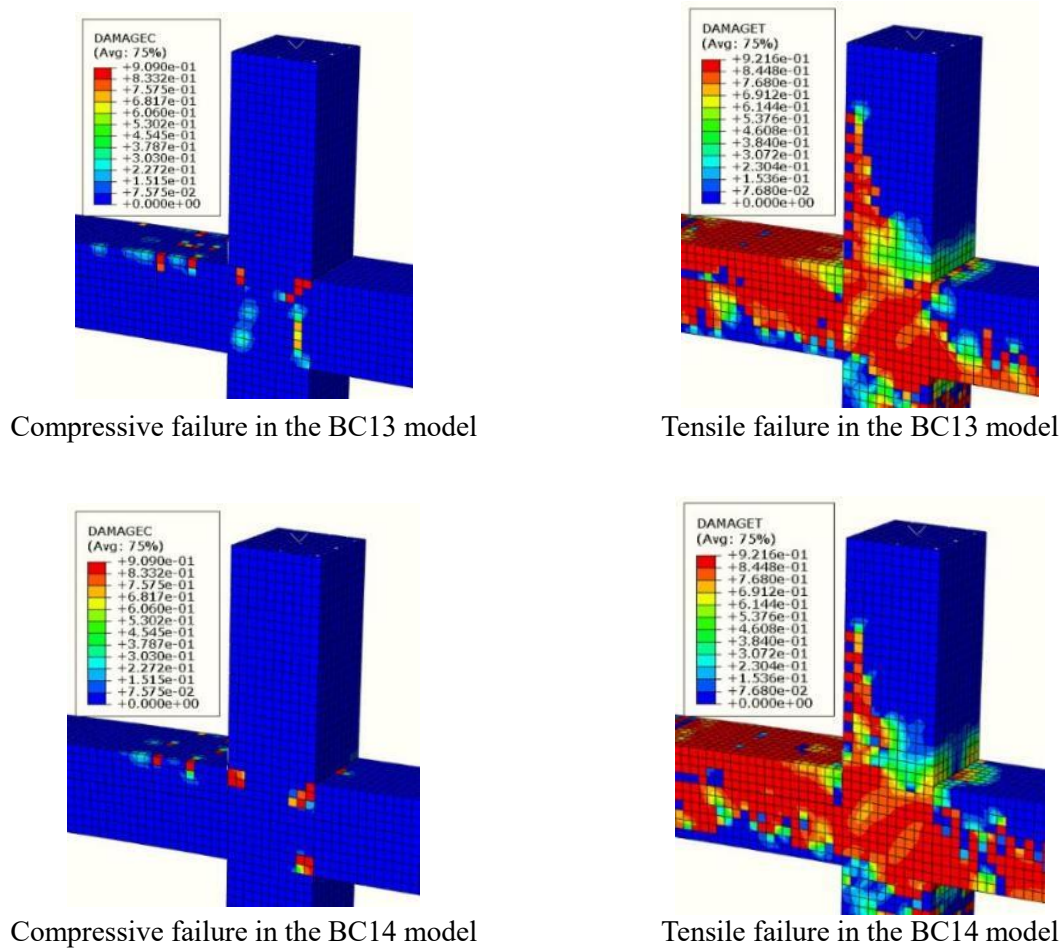
Compressive failure in the BC13 model

Tensile failure in the BC13 model

Compressive failure in the BC14 model

Tensile failure in the BC14 model

Fig. 17. Cracking pattern of the numerical models of BC13 and BC14.

The displacement ductility is deliberated in the current study. The ductility values are calculated in accordance to the displacement at the yield state (Δy) (a stage where the first yield of reinforcement steels occurs at the connection zone), and ultimate displacement is calculated at the failure state (Δu). The displacement corresponding to 80% reduction of the ultimate load bearing capacity is contemplated as Failure state displacement. Figure 18 compares the ductility values in the numerical models the maximum and minimum ductility are related to the BC3 and BC5 models, respectively.
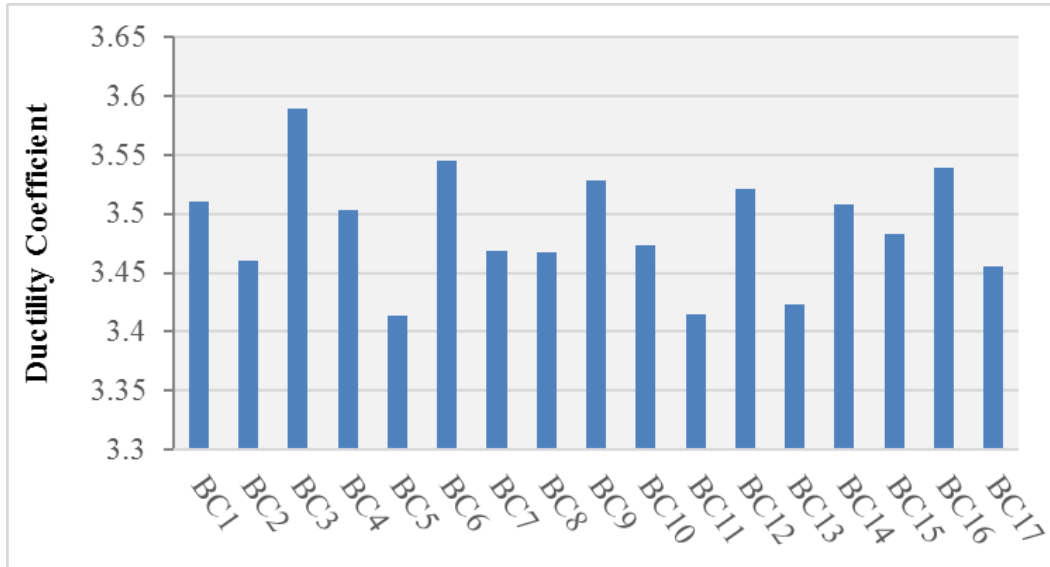
Fig. 18. Ductility of the numerical models.

Figure 19 compares the rigidity of the elastic region of the load-displacement envelope of the numerical models. As the rigidity of the connection zone increases, the displacement values are decreased, so the higher rigidity leads to the lower ductility.
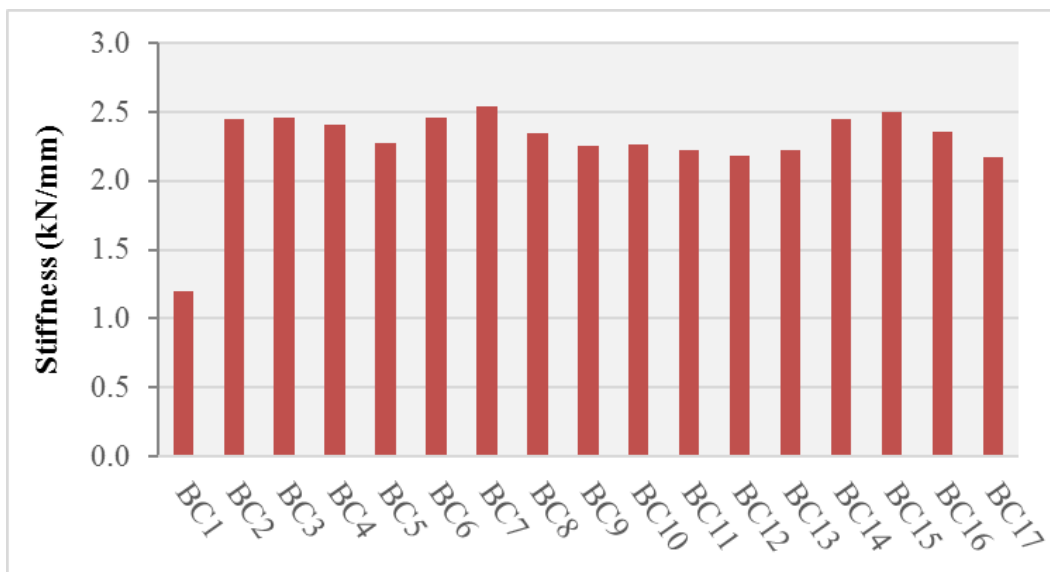

Fig. 19. Rigidity of the numerical models.

The energy dissipation of connections depends on the area-under-the-curve of load-displacement diagram after each loading cycle. Figure 20 displays the values of energy dissipation in various models. The minimum and maximum energy dissipation belong to the BC1 and BC9 models, respectively.
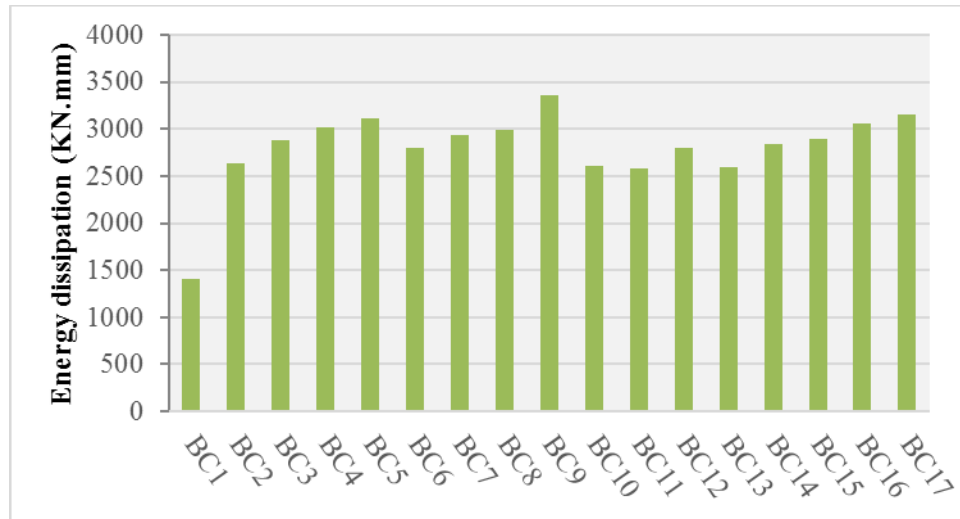
Fig. 20. Energy dissipation of the numerical models.

The response modification factor of precast connections is calculated pursuant to the overstrength coefficient, ductility coefficient, redundancy coefficient, and damping coefficient. These coefficients are calculated using the slopes of the equivalent

three linear envelope diagrams in the elastic and plastic regions. The 2D clustered column bar of Figure 21 presents the comparison of the response modification factor of the studied models.
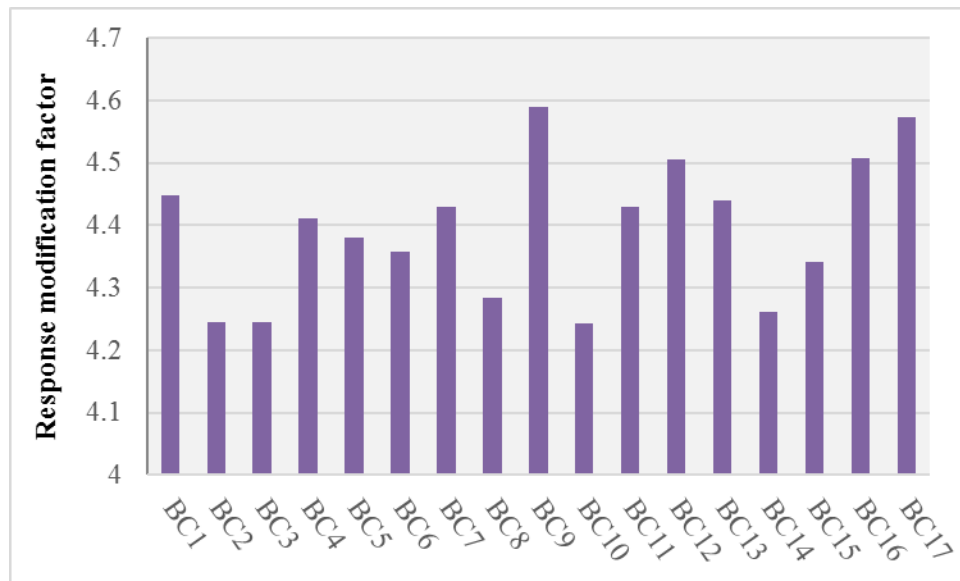
Fig. 21. Response modification factor of the numerical model.

The numerical models were classified into four groups to facilitate the parametric study of the variable of ductility, rigidity, energy dissipation, and response modification factor. Group "A" includes couplers at constant distance from column face, and the grout

compressive strength of 30 MPa (Models BC2, BC4, BC5, BC6, BC8, BC9). As the compressive strength of them are equal, the effect of axial load, stirrup distance, and coupler distance from the column face can be obtained on the noted variables. Group B is

similar to Group A with the grout compressive strength of 35 MPa (Models BC3 and BC7). So, the effect of increasing grout compressive strength can be determined through comparing the results of this group with the Group A. The main characteristic of the Group C is the overlap splices in the bottom layer of the beam (Models: BC10, BC11, BC12, BC13). The effects of the overlap splices can be evaluated upon comparing this group with Group A. Group D consists of couplers in the various distances from the column face (Models: BC14, BC15, BC16, BC17). Group O includes the control model with no couplers and grout.

In terms of ductility, the comparison of the models in Group A reveals that the reduction of couplers' distance from the column face improves the ductility by 3.5%. In addition, the effect of stirrup distance reduction is negligible and fall in a negative region. The comparison of the Groups A and D indicates that the grout compressive strength is higher meaningful in the models with the couplers farther from the column face. Comparison of Group C with A and D proves that the use of overlap splices in the lower layer is disadvantageous for seismic behavior of the connection zone.

The compressive strength of the grout is the most influential parameter in the rigidity factor of the models. The rigidity of the precast models is much higher than that of the monolithic observant one.

The simultaneous effect of the load-bearing capacity and ductility can be observed in the energy dissipation variations. In comparison the Groups A and D, it is concluded that the models with a coupler-column distance of 5 cm provide a higher energy dissipation about 6% in relation to the models with combined and 20cm distance. This fact demonstrates the ability of the couplers in creating further strength and continuity in the bars. Thus, the load-bearing capacity of the beam in the vicinity of the connection zone is markedly increased by enhancing bar strength and diameter at the noted region. As it can be stated in the comparison of the groups A and D, the reduction of the stirrup distances leads to a 16% increase in the energy dissipation. In the comparison of the Groups A and C, the negative (6%) effect of lower overlap splices in reduction of the energy dissipation becomes evident. The increase of the grout compressive strength leads to a 6% the increase in energy dissipation.

Response modification factor can reveal the effect of all the noted variables in the value of the force required to design the connection. The comparison of Groups A and D proves that the models with a 5cm coupler-column distance have a 6% higher response modification factor than those with a 20cm distance, and this value is decreased to 3% in the case with combined coupler arrangements. These variations are similar to those observed in the case of energy dissipation. The reduction of the stirrup distances provides the maximum effect, leading to an 8.2% increase in the response modification factor. In comparison of Groups A with Group C, the negative effect of the lower overlap splices is less than 3%. In contrast to the energy dissipation variable, the gout compressive strength provides a little effect on the response modification response.

6. Conclusions

The precast rigid connections are of utmost significance in the seismic regions. Generally, the seismic behavior of the connection zone is carried out in the terms of

the ductility, rigidity, lateral load-bearing capacity, energy dissipation, and response modification factor. Several numerical models were prepared to study the precast connection zone. The numerical analysis method was verified through the test results. The following conclusions can be drawn based on the statistical analysis of the numerical study results.

The couplers implementation, particularly the ones placed close to column face ameliorates the connection zone seismic behavior. The use of grout with higher compressive strength is recommended for the proposed semi-dry precast connections.

The crack propagation pattern is similar to the monolithic constructed connection zone. The flexural cracks are initiated in the beams and developed to about half of the beam, after about four cycles of loading (the elastic region), shear cracks are appeared in the connection zone, the flexural cracks are appeared in the length of about 1/3 to 1/5 of the column height.

The main source of the energy dissipation is the movements of the beam-column connection zone as a result of the discontinuities of the noted region. However, the initial strain was appeared in the connection zone, no strain occurred on the top of the beam at the location of the couplers.

The compressive strength of the grout is the most effective parameter in the connection zone rigidity.

The numerical results demonstrate that the reduction of the stirrup distances is the main parameter in order to improve the energy dissipation and the response modification factor. Therefore, the closest coupler to the column face and minimum distance of the stirrups establishes the most optimized connection zone in the domain of the studied cases.

REFERENCES

[1] Park, R., & Thompson, K. J. (1977). Cyclic load tests on prestressed and partially prestressed beam-column joints. PRECAST/PRESTRESSED CONCRETE INSTITUTE. JOURNAL, 22(5).

[2] Bull.D.K. and Park.R. (1986) "Seismic Resistance of Frames Incorporating Precast Prestressed Concrete Beam Shells". PCI Journal. V.B1.NO.4. PP.54-93

[3] Pillai.S.U. and Kirk.D.W. (1981) "Ductile Beam-Column Connection in Precast Concrete". ACI Structural Journal. V.78 No.6, PP.480-487.

[4] Bhatt.P and Kirk.D.W. (1985) "Tests on an improved Beam-Column connction for precast concrete". ACI Structural Journal V.82 NO.6. PP.834-843.

[5] Sekin.M. and Fu.H.C. (1990) "Beam-Column Connection in Precast Reinforced Concrete Construction". ACI Structural Journal V.87.NO3.PP252-261.

[6] Stanon.J.F., Anderson.R.G., Dolan.c.w. and Mc Cleary.D. E (1986) "Moment Resistant Connection and Simple Connections". Research project NO.1/4. Precast/Prestressed Concrete Institute. Chicago.

[7] Tankat.A.T., Ersoy.U and Ozacebe.G.(1998)" seismic performance of Precast Concrete Connection", The 11th European Conference on Earthquake Engineering. Balkema, Austria. PP.30-37.

[8] Khaloo.A.R. and Parastesh.H.(2003) "Cyclic Loading of Ductile Precast Concrete Beam-Column Connection". ACI Structural Journal. V.100. NO.3. PP.291-296

[9] Khaloo.A.R. and Parastesh.H.(2003) "Cyclic Loading Response of simple Moment-Resisting Precast Concrete Beam-Column

Connection". ACI Structural Journal. V.100. NO.4. PP.440-445

[10] Parastesh.H., Khaloo.A. R & Ramezani.R. "Experimental Study of Interior Connection in Prefabricated R/C Frames". Submitted to Engineering Structures.

[11] Parstesh H., Mobedi E., Ghasemi H. Amjadian, K. (2019), "Experimental Study for Strength Capacity of Cold-Formed Steel Joists Connections with Consideration of Various Bolts Arrangements", 7(2), 61-70.

[12] Sudhakar.A. Kulkarni, Bini Li, Woon Kwong Yip (2007) "Finite element analysis of precast hybrid-steel concrete connection under cyclic loading" Journal of Constructional Steel Research.

[13] Guan, D., Guo, Z., Jiang, C., Yang, S., & Yang, H. (2018). Experimental evaluation of precast concrete beam-column connections with high-strength steel rebars. KSCE Journal of Civil Engineering, 1-13.

[14] Bahrami, S., Madhkhan, M., Shirmohammadi, F., & Nazemi, N. (2017). Behavior of two new moment resisting precast beam to column connections subjected to lateral loading. Engineering Structures, 132, 808-821.

[15] Fathi, M., Parvizi, M., Karimi, J., & Afreidoun, M. H. (2018). Experimental and numerical study of a proposed moment-resisting connection for precast concrete frames. Scientia Iranica, 25(4), 1977-1986.

[16] Xiao, J., Ding, T., & Zhang, Q. (2017). Structural behavior of a new moment-resisting DfD concrete connection. Engineering Structures, 132, 1-13.

[17] Yan, Q., Chen, T., & Xie, Z. (2018). Seismic experimental study on a precast concrete beam-column connection with grout sleeves. Engineering Structures, 155, 330-344.

[18] Alias, A., Zubir, M. A., Shahid, K. A., & RAhman, A. B. A. (2013). Structural performance of grouted sleeve connectors with and without transverse reinforcement

for precast concrete structure. Procedia Engineering, 53, 116-123.

[19] Clementi, F., Scalbi, A., & Lenci, S. (2016). Seismic performance of precast reinforced concrete buildings with dowel pin connections. Journal of Building Engineering, 7, 224-238.

[20] Nzabonimpa, J. D., Hong, W. K., & Kim, J. (2017). Nonlinear finite element model for the novel mechanical beam-column joints of precast concrete-based frames. Computers & Structures, 189, 31-48.

[21] Girgin, S. C., Misir, İ. S., & Kahraman, S. (2017). Seismic performance factors for precast buildings with hybrid beam-column connections. Procedia engineering, 199, 3540-3545.

[22] Bompa, D. V., and A. Y. Elghazouli. (2019), "Inelastic cyclic behavior of RC members incorporating threaded reinforcement couplers." Engineering Structures 180: 468-483.

[23] Woon, Kai-Siong, and Farzad Hejazi. (2019), "Vertical Cyclic Performance of Precast Frame with Hook-end U-shaped High-damping Rubber Joint." KSCE Journal of Civil Engineering: 1-12.

[24] Hibbitt, Karlson&Sorensen Inc. (2005) ABAQUS/standard user's manual, Version 6.5. Providence (RI).

[25] Mander J.B., Priestley M.J.N., Park R (1988). "Theoretical stress-strain, Vol. 114, No. 8, pp. 1804-1826

[26] Sargin.M. (1971) "stress-strain Relationships for concrete and the analysis of structural concrete sections.", university of waterloo.

[27] Ab-Kadir, Mariyana A., et al. (2014), "Experimental and Numerical Study on Softening and Pinching Effects of Reinforced Concrete Frame." IOSR Journal of Engineering 4.5: 1.